

Electronic Supporting Information

Near-Infrared Vapochromism in Lipid-Packaged Mixed-Valence Coordination Polymers

Yuki Nagai,^a Masa-aki Morikawa^{ab} and Nobuo Kimizuka^{*ab}

^a Department of Chemistry and Biochemistry, Graduate School of Engineering, Kyushu University, 744 Moto-oka Nishi-ku, Fukuoka 819-0395, Japan.

^b Center for Molecular Systems (CMS), Kyushu University, 744 Moto-oka Nishi-ku, Fukuoka 819-0395, Japan.

E-mail: n-kimi@mail.cstm.kyushu-u.ac.jp

[General methods]

Identification of compounds:

¹H-NMR spectroscopy was performed on a Bruker DRX-300 spectrometer (300 MHz). FT-IR (ATR) spectroscopy was performed a Shimadzu IRTracer-100 with a Smith Detection DuraSamplIR II as the ATR accessory. Elemental analysis (EA) was conducted at the Elemental Analysis Center, Kyushu University.

UV-Vis-NIR spectroscopy:

UV-Vis-NIR spectroscopy was performed on either a JASCO V-670 spectrophotometer or a JASCO V-770 spectrophotometer. Spectra for powder (Fig. 1, Fig.2) were obtained by the diffuse reflectance method. The UV-Vis-NIR spectra of the cast film (Fig. S3, Fig. S13) were measured by the usual transmission method. The spectra of solutions (Fig. S4) were recorded at 25 °C using a quartz cuvette with a 1-mm path length.

Raman spectroscopy:

Raman spectroscopy was performed on a JASCO NRS-3100 using a 532 nm laser.

X-ray diffraction:

Powder X-ray diffraction (PXRD) measurements were performed on a Bruker D2 Phaser with Cu K_α irradiation ($\lambda = 1.5406 \text{ \AA}$). Grazing-incidence small-angle X-ray scattering (GI-SAXS) was performed in a Rigaku NANO-Viewer small-angle X-ray scattering system equipped with a PILATUS 100K pixel detector, and Cu K_α irradiation ($\lambda = 1.5406 \text{ \AA}$) was provided by a microfocus sealed tube operating at 40 kV, 30 mA. Temperature control in GI-SAXS was performed using a temperature control stage, LINKAM 10033L.

Thermogravimetry (TG):

TG was performed on a Rigaku thermo plus EVO2 TG8121.

Differential scanning calorimetry (DSC):

DSC was performed on a METTLER TOLEDO Excellence DSC 1.

Quartz crystal microbalance (QCM):

QCM measurements were performed on QCM922A (SEIKO EG&G CO., LTD.) with QCM resonators PSA-SL-0901T (Frequency: 9.176 MHz, Electrode area: 0.1963 cm², NIHON DEMP KOGYO CO., LTD.). ca. 1mg of lipid complex [Pt^{II}(en)₂][Pt^{IV}(en)₂I₂](I)₄ was dispersed in chlorocyclohexane (1 ml) and the dispersion (several tens of μ l) was cast on QCM resonators followed by drying in a desiccator under reduced pressure. Before the exposure to MeOH vapor, the drift in frequency settled down approximately in 100 seconds. Typically, the weight of the cast film was calculated as 14.57 μ g from the frequency change from 9,172,040 MHz to 9,157,892 MHz before and after the drop-casting. The cast film weight was used as a reference to calculate weight changes (%) in the graphs shown in Fig. S8. In 20 ml sample bottles, a few ml of MeOH or water was placed, and the QCM resonator was

inserted through the sample bottle opening. The measurement was started immediately at room temperature. When the QCM resonator was exposed to MeOH, the opening of the sample bottle was sealed by parafilm.

The weight changes were calculated according to the Sauerbrey equation, using the quartz shear modulus of $2.947 \times 10^{11} \text{ g cm}^{-1} \text{ s}^{-2}$ and the quartz density of 2.648 g cm^{-3} .¹

[Materials]

L-glutamic acid, 1-dodecanol, sodium carbonate, hydrochloric acid (35%), sodium hydrogen carbonate, and perchloric acid (70%) were purchased from Kishida Chemical Co., Ltd. *p*-Toluenesulfonic acid (PTS) monohydrate, toluene, chloroform, anhydrous sodium sulfate, acetone, triethylamine, *N,N*-dimethylformamide (DMF), BOP reagent, sodium chloride, ethyl acetate, methanol, ethylenediamine, and ethanol were purchased from FUJIFILM Wako Pure Chemical Corporation. Sulfoacetic acid was purchased from Sigma-Aldrich. Potassium tetrachloroplatinate(II) was purchased from Kojima Chemicals Co., Ltd. Iodine was purchased from Kanto Chemical Co., Inc. 1-Dodecanol was purified by distillation before using, and the other chemicals were used as received. The water used in this report was purified with a Direct-Q system (Millipore Co.) and had a resistivity higher than 18.2 MΩcm.

[Preparation of cast films and vapochromism experiments]

$[\text{Pt}(\text{en})_2][\text{Pt}(\text{en})_2\text{I}_2](\mathbf{1})_4$ was dispersed in chlorocyclohexane by using a bath-type ultrasonicator.

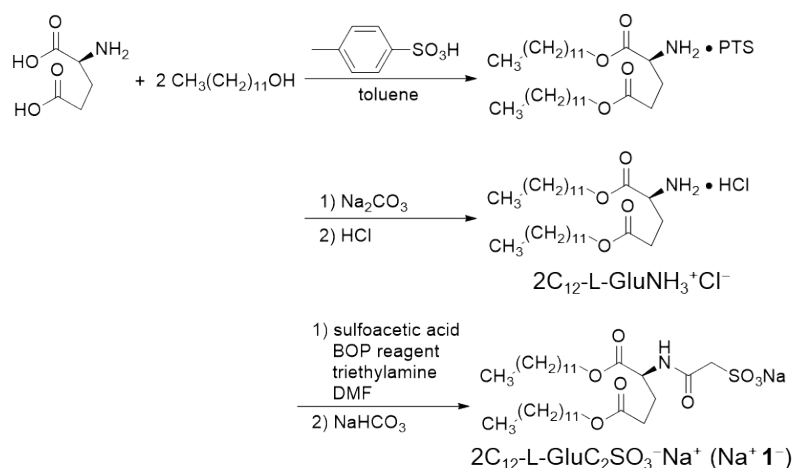
Cast films of $[\text{Pt}^{\text{II}}(\text{en})_2][\text{Pt}^{\text{IV}}(\text{en})_2\text{I}_2](\mathbf{1})_4$ were prepared by casting chlorocyclohexane dispersions of $[\text{Pt}(\text{en})_2][\text{Pt}(\text{en})_2\text{I}_2](\mathbf{1})_4$ on a quartz plate, followed by drying in vacuo.

In methanol-induced vapochromism experiments, a small sample table was placed in a petri dish, and the pristine compound $[\text{Pt}(\text{en})_2][\text{Pt}(\text{en})_2\text{I}_2](\mathbf{1})_4$ or its cast film was placed on it. The petri dish was filled with a small amount of methanol which was separated from the specimen, and the lid of the petri dish was placed on the top. The methanol vapor slowly diffused into the sample on the sample stand, and the powder turned reddish-brown after several hours at room temperature. This color change was accelerated by heating the specimen at 40 °C just for a few minutes.

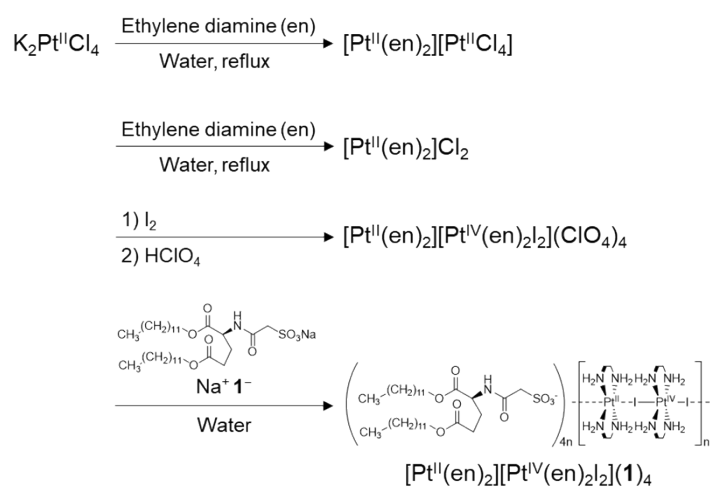
The reddish-brown samples formed by the methanol vapor treatment returned to their original indigo color upon contact with water vapor. The reddish-brown powder on a sample holder was placed in a petri dish containing a small amount of water, and when the lid of the petri dish was put on, the color of the sample returned to its original indigo color at room temperature in a few minutes.

[Synthesis]

The complex $[\text{Pt}^{\text{II}}(\text{en})_2][\text{Pt}^{\text{IV}}(\text{en})_2\text{I}_2](\mathbf{1})_4$ was synthesized according to Scheme S1 and S2, based on our previous report.²



Scheme S1. Synthesis scheme of the anionic lipid $\text{Na}^+ \mathbf{1}^-$.



Scheme S2. Synthesis scheme of the lipid complex $[\text{Pt}^{\text{II}}(\text{en})_2][\text{Pt}^{\text{IV}}(\text{en})_2\text{I}_2](\mathbf{1})_4$.

Synthesis of $2\text{C}_{12}\text{-L-GluNH}_3^+\text{Cl}^-$:

L-glutamic acid (10.0 g, 68.0 mmol), 1-dodecanol (28.0 g, 150 mmol), *p*-toluenesulfonic acid (PTS) monohydrate (20.0 g, 105 mmol) were dissolved in toluene (120 ml) and refluxed for 7 h using a Dean-Stark apparatus. After solvent evaporation, the residue was dissolved in chloroform and washed with saturated sodium carbonate aqueous solution. After checking that the aqueous layer is basic, the organic layer was dried with anhydrous sodium sulfate. The residue after filtering sodium sulfate out and evaporating the solvent was dissolved in acetone (240 ml). To the solution cooled in an ice bath, concentrated hydrochloric acid (68.0 mmol) was slowly added, which gave colorless precipitate. The precipitate was filtered and recrystallized from acetone to give colorless crystals. Yield: 27.45 g (77.6%). FT-IR (cm^{-1}): ν (C=O) 1742, ν (O=C-O-C) 1215. ^1H NMR (DMSO- d_6 , 300 MHz): δ 0.86 (m, 6H); δ 1.25 (m, 36H); δ 1.57 (m, 4H), δ 2.04 (dt, 2H), δ 2.51 (m, 1H), δ 4.03 (m, 3H), δ 4.14 (m, 2H), δ 8.43 (s, 3H).

Synthesis of $2\text{C}_{12}\text{-L-GluC}_2\text{SO}_3^-\text{Na}^+ (\text{Na}^+ \mathbf{1}^-)$:

Sulfonic acid (3.10 g, 22.1 mmol) and triethylamine (5.86 g, 57.9 mmol) in DMF (160 ml) were added to 2C_{12} -

L-GluNH₃⁺Cl⁻ (10.7 g, 20.6 mmol) and triethylamine (2.07 g, 20.5 mmol) in DMF (75 ml). To the solution cooled in an ice bath, BOP reagent (13.7 g, 31.0 mmol) in DMF (25 ml) was slowly added, and the mixture was stirred for 4 days at room temperature. After solvent evaporation, the residue was dissolved in chloroform. The solution was washed with saturated brine and then saturated sodium hydrogen carbonate aqueous solution. The organic layer was dried with anhydrous sodium sulfate. After removing sodium sulfate by filtration, the filtrate was condensed by solvent evaporation. The condensed liquid was added to ethyl acetate to form a precipitate. The precipitate was filtered and recrystallized from methanol to give colorless powder. Yield: 6.60 g (51.4%). FT-IR (cm⁻¹): ν (N-H) 3291, ν (ester C=O) 1734, ν (amide C=O) 1653, δ (N-H) 1537, ν (O=C-O-C) 1206. ¹H NMR (chloroforms-d₁, 300 MHz): δ 0.88 (m, 6H); δ 1.26 (m, 36H); δ 1.59 (m, 4H), δ 2.03 (m, 1H), δ 2.17 (m, 1H), δ 2.41 (dd, 2H), δ 4.02 (m, 6H), δ 4.53 (dd, 1H), δ 7.97 (s, 1H). EA (%): Calcd. for C₃₁H₅₈NNaO₈S: C, 59.30; H, 9.31; N, 2.23. Found: C, 58.74; H, 9.25; N, 2.25.

Synthesis of [Pt^{II}(en)₂]Cl₂:

Potassium tetrachloroplatinate(II) (0.500 g, 1.20 mmol) was dissolved in water. To the solution under reflux was added excess ethylenediamine (0.516 g, 8.59 mmol) to give a precipitate. Reflux was continued until the precipitate was dissolved, and the solution was cooled to room temperature and neutralized using dilute hydrochloric acid (~0.1 M). To the neutralized solution was added potassium tetrachloroplatinate(II) (0.500 g, 1.20 mmol) to give a pale purple precipitate. The precipitate was filtered and suspended in water (30 ml). To the suspension was added excess ethylenediamine (1.27 g, 21.1 mmol). The suspension was heated until it got a transparent solution by dissolving the precipitate. After hot filtration, the filtrate was condensed by solvent evaporation. To the condensed solution was added an ethanol/acetone mixture (1/1, v/v) (30 ml). The formed precipitate was filtrated to give colorless powder. Yield: 0.598 g (64.3%). EA (%): Calcd. for C₄H₁₆Cl₂N₄Pt: C, 12.44; H, 4.18; N, 14.51. Found: C, 12.44; H, 4.16; N, 14.39.

Synthesis of [Pt^{II}(en)₂][Pt^{IV}(en)₂I₂](ClO₄)₄:

Iodine (0.335 g, 1.32 mmol) dissolved in ethanol (20 ml) was added to [Pt^{II}(en)₂]Cl₂ (1.02 g, 2.64 mmol) dissolved in water (20 ml). To the mixture was added perchloric acid to form a deep green precipitate. The precipitate was filtered to give brownish-green powder. Yield: 1.55 g (91.6%). EA (%): Calcd. for C₈H₃₂Cl₄I₂N₈O₁₆Pt₂: C, 7.49; H, 2.52; N, 8.74. Found: C, 7.63; H, 2.55; N, 8.36.

Synthesis of [Pt^{II}(en)₂][Pt^{IV}(en)₂I₂](I)₄:

The anionic lipid Na⁺I⁻ (502 mg, 0.800 mmol) was dispersed in water (20 ml) using a probe sonicator (Branson, Digital Sonifier 250D Advanced). To the dispersion was added [Pt^{II}(en)₂][Pt^{IV}(en)₂I₂](ClO₄)₄ (256 mg, 0.200 unit mol) dissolved in water (80 ml) by heating. The mixture was stirred for 146 h at room temperature to form a precipitate. The precipitate suspension was centrifugated (1 °C, 10000 rpm, 20 min) using a centrifuge (TOMY, MX-205). After centrifugation, the supernatant was carefully decanted. A series of operations of water addition, centrifugation, and decantation were repeated two times. Finally, the precipitate was dried under a vacuum to give indigo powder. Yield: 286 mg (43.3%). EA (%): Calcd. for C₁₃₂H₂₆₈I₂N₁₂O₃₄Pt₂S₄ (Dihydrate): C, 47.47; H, 8.09;

N, 5.03. Found: C, 47.62; H, 8.14; N, 5.03.

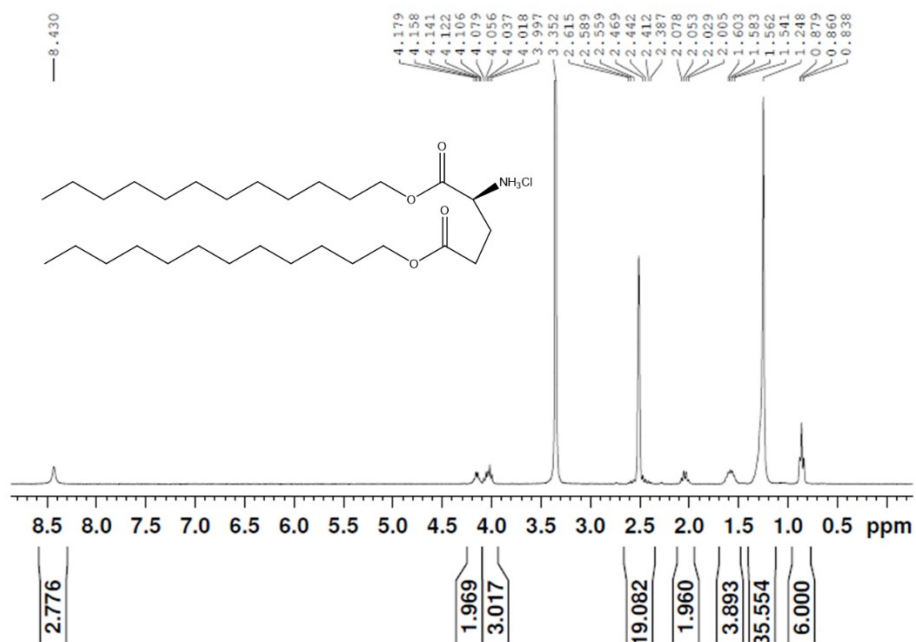


Fig. S1 ¹H-NMR spectrum of the lipid 2C₁₂-L-GluNH₃⁺Cl⁻ (DMSO-d₆, 300 MHz).

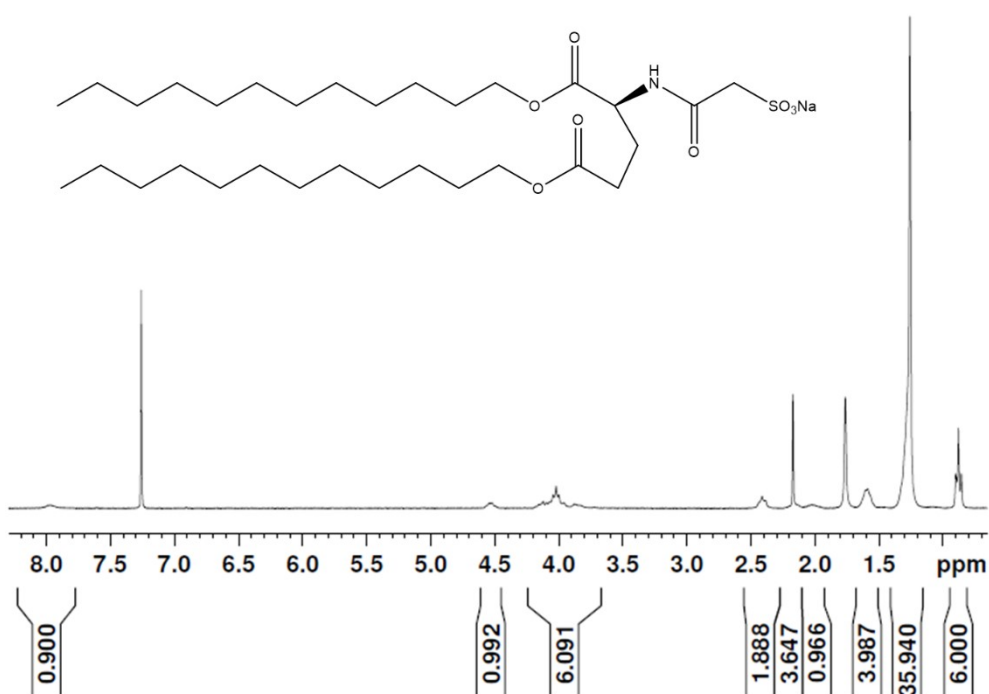


Fig. S2 ¹H-NMR spectrum of the lipid Na⁺1⁻ (Chloroform-d₁, 300 MHz).

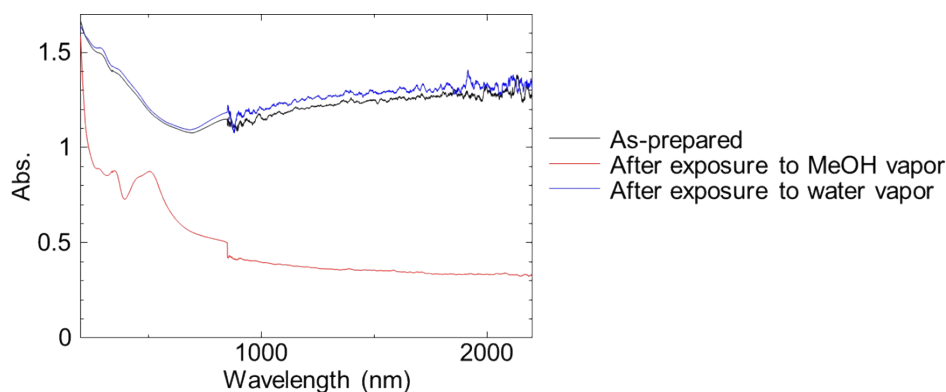


Fig. S3 UV-Vis spectrum changes of the cast film $[\text{Pt}(\text{en})_2][\text{Pt}(\text{en})_2\text{I}_2](\mathbf{1})_4$ at room temperature.

Black line: as-prepared sample, red line: after exposure to MeOH vapor, blue line: after exposure to water vapor. These spectra were obtained by the transmission method.

As mentioned in the text, the as-synthesized indigo-colored powder sample exhibits a continuous broad absorption spectrum from the visible region to over 2,000 nm (E_{CT} less than 0.6 eV, Fig. 2a, Fig. S3). This CT band is dramatically red-shifted from the crystalline perchlorate complex $[\text{Pt}(\text{en})_2\text{I}_2][\text{Pt}(\text{en})_2](\text{ClO}_4)_4$ (CT absorption around 905 nm (1.37 eV)),³ as a result of enhanced metal-metal interactions directed by densely packed lipid counteranions.^{2,4} The observed IVCT band is remarkably small for iodo-bridged Pt complexes and comparable to the smallest E_{CT} value reported to date (0.53 eV) at room temperature.^{2,3} It indicates that dense packing of sulfonate groups of the lipid molecules reduces the distance between $\text{Pt}(\text{en})_2$ complexes in the 1D chains, thus increasing metal-metal interactions.^{2,4,5} The exceptionally small E_{CT} led to the expectation that the iodide ions are positioned close to the center of the one-dimensional $\text{Pt}(\text{en})_2$ complex that ultimately provides an averaged valence (AV), i.e., -I-Pt(III)-I-Pt(III)- state. This is also consistent with the single $\nu(\text{N-H})$ band observed for the ethylenediamine (en) ligands of the indigo-colored complex shown in Fig. S10 (ESI).

Meanwhile, in a Raman spectrum of the as-synthesized powdery $[\text{Pt}(\text{en})_2][\text{Pt}(\text{en})_2\text{I}_2](\mathbf{1})_4$, a peak assigned to the Pt-I stretching mode $\nu(\text{Pt-I})$ ^{6,7} was observed at 128 cm^{-1} (i, Fig. 2b). As symmetric Pt-I stretching mode $\nu(\text{Pt-I})$ is considered as Raman-inactive, the coordination environment around the iodide anion is rather asymmetric, i.e., iodide anions slightly deviate from the midpoint of the Pt-I-Pt units toward the Pt(IV) complex. These results indicate that the electronic structure of the complex $[\text{Pt}(\text{en})_2][\text{Pt}(\text{en})_2\text{I}_2](\mathbf{1})_4$ is in the boundary region between the average valence (AV) state and the mixed-valence state. Although the electronic structure of the indigo-colored, lipid complex $[\text{Pt}(\text{en})_2][\text{Pt}(\text{en})_2\text{I}_2](\mathbf{1})_4$ is close to the averaged valence structure as a result of the enhanced Pt-Pt interactions by lipid counterions, it is not a perfect average valence (AV) state and it is more of a mixed-valence state due to the large lattice - electronic interactions (S) of the one-dimensional Pt complexes.⁸

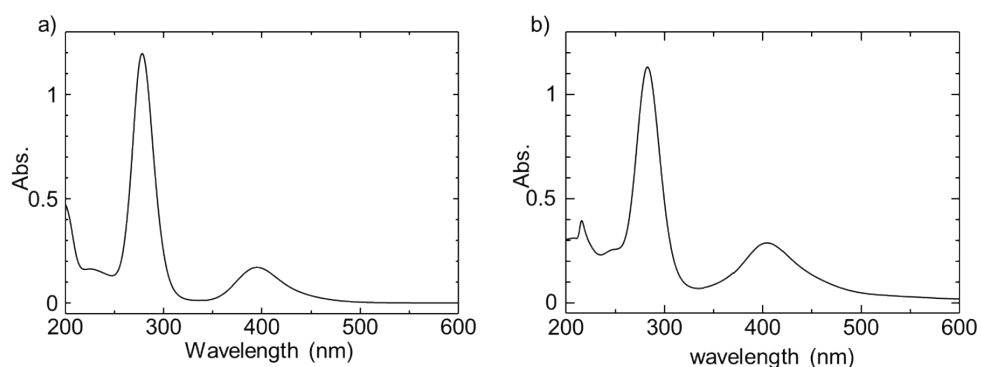


Fig. S4 UV-Vis spectra of dissociated (monomerically dissolved) platinum complexes in solvents (0.3 unit mM, 25 °C, 1 mm cuvette). a) $[\text{Pt}(\text{en})_2][\text{Pt}(\text{en})_2\text{I}_2](\text{ClO}_4)_4$ in water. b) the complex $[\text{Pt}(\text{en})_2][\text{Pt}(\text{en})_2\text{I}_2](\mathbf{1})_4$ in dichloromethane.

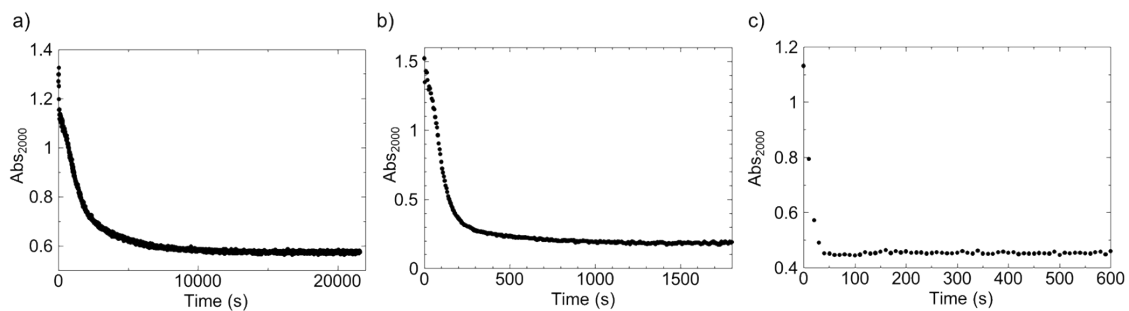


Fig. S5 Time-dependences of absorption at 2000 nm (Abs_{2000}) after exposure of cast films $[\text{Pt}(\text{en})_2][\text{Pt}(\text{en})_2\text{I}_2](\mathbf{1})_4$ to methanol vapor at different temperatures. a) 25 °C, b) 35 °C, c) 45 °C.

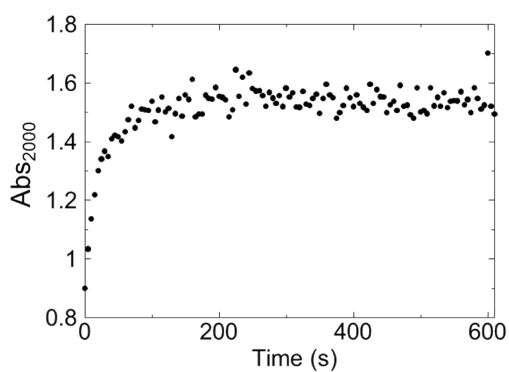


Fig. S6 Time-dependence of the Abs_{2000} of MeOH-treated cast film $[\text{Pt}(\text{en})_2][\text{Pt}(\text{en})_2\text{I}_2](\mathbf{1})_4$ upon exposure to water vapor at 25 °C. The change was too rapid to trace its initial step.

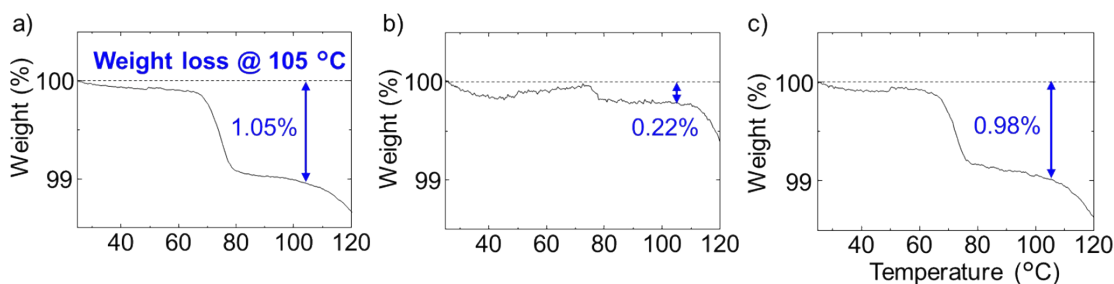


Fig. S7 TG curves of the complex $[\text{Pt}(\text{en})_2][\text{Pt}(\text{en})_2\text{I}_2](\mathbf{1})_4$ powder (scan rate: $10\text{ }^\circ\text{C}/\text{min}$), a) as-synthesized, b) after exposure to MeOH vapor, c) after exposure to water vapor.

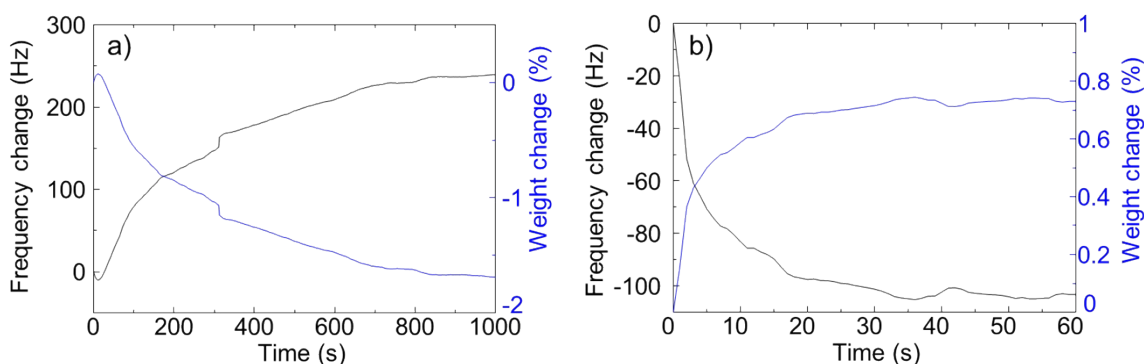


Fig. S8 Time-dependence of the frequency changes of QCM at room temperature. A cast film of $[\text{Pt}(\text{en})_2][\text{Pt}(\text{en})_2\text{I}_2](\mathbf{1})_4$ ($14.57\text{ }\mu\text{g}$) was prepared on a QCM resonator. fundamental frequency, 9.176 MHz . a) Time dependence after the film on QCM resonator was exposed to MeOH vapor. b) Time dependence after exposure of MeOH-vapor-treated film to water vapor.

After exposure to MeOH vapor, a weight decrease of $\sim 1.7\%$ was observed for the film cast on the QCM resonator in ca. 17 min. This weight decrease is roughly equal to the theoretical water amount of the dihydrate complex ($\sim 1.08\%$). It confirms that the elimination of water of crystallization occurs facily in the MeOH-vapor atmosphere. The time required for crystallization water elimination will depend on parameters such as the thickness and area of the films and temperature. Meanwhile, subsequent exposure to water vapor caused a rapid weight increase of $\sim 0.8\%$, indicating the uptake of water of crystallization. The observed amount of water seems to be underestimated because the rapid hydration occurred for several seconds before starting the measurement.

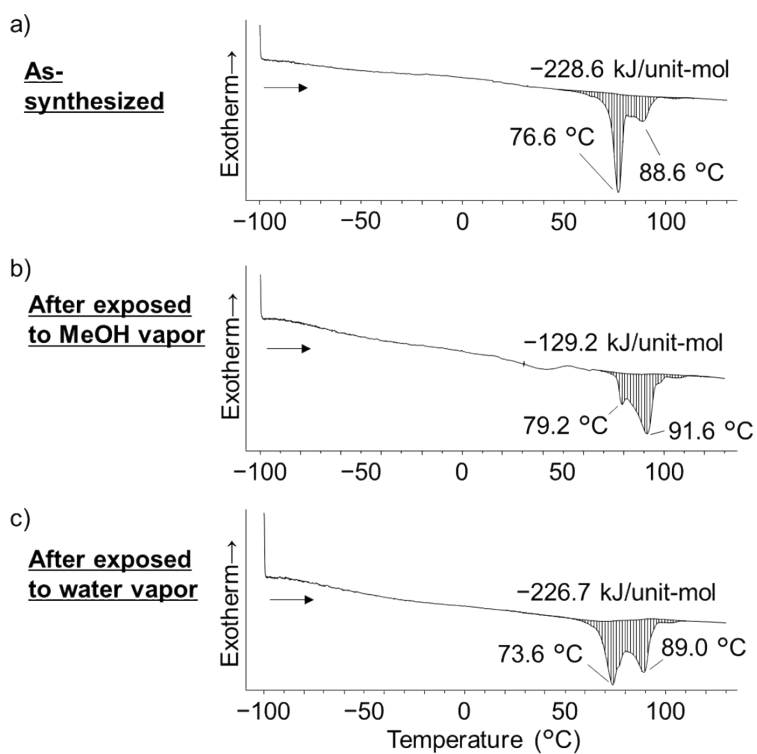


Fig. S9 DSC curves of the powdery $[\text{Pt}(\text{en})_2][\text{Pt}(\text{en})_2\text{I}_2](\mathbf{1})_4$ (scan rate: 2 °C/min), a) as-synthesized, b) after exposed to MeOH vapor, c) After exposed to water vapor.

The as-synthesized complex $[\text{Pt}(\text{en})_2][\text{Pt}(\text{en})_2\text{I}_2](\mathbf{1})_4$ shows endothermic peaks around 77 °C, which would reflect the crystal-to-liquid crystal phase transition of lipid molecules in the sample. We note that the prominent DSC peak after exposure to methanol vapor has been changed to 91.6 °C (Fig. S9b), indicating alteration of the molecular orientation of lipid molecules caused by the methanol-induced dehydration process.

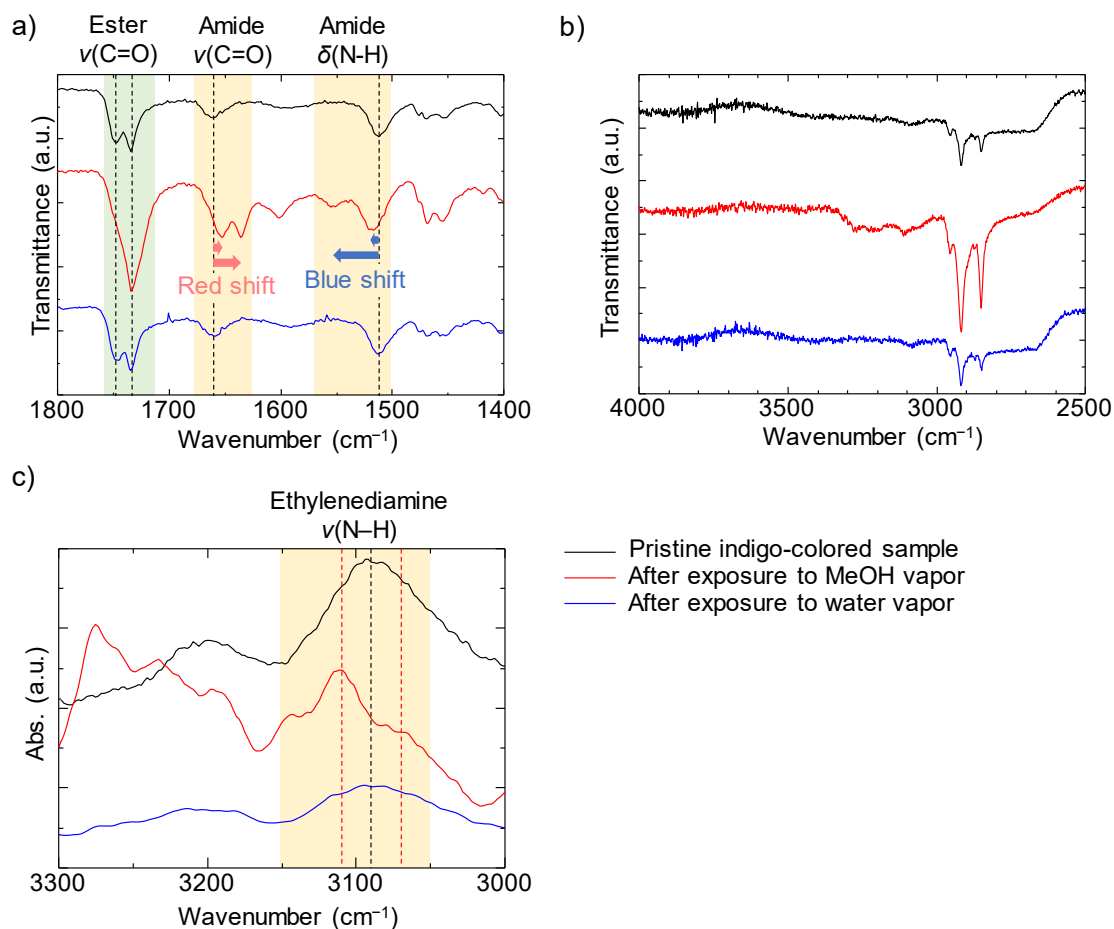


Fig. S10 FT-IR spectral changes of the powdery complex $[\text{Pt}(\text{en})_2][\text{Pt}(\text{en})_2\text{I}_2](\mathbf{1})_4$ in concert with vapochromism. All the spectra were obtained by the attenuated total reflection method at room temperature. a) spectral range from 1400 to 1800 cm^{-1} , b) spectral range from 2500 to 4000 cm^{-1} , c) spectral range of 3000 to 3300 cm^{-1} . In c), the vertical axis is shown as absorbance to clearly show spectral changes. Changes of FT-IR spectra in a) are discussed in the main text.

No significant spectral changes except for the 3000–3300 cm^{-1} range are observed in b), because of the small crystallization water contained in the sample. The peaks in the range of 3050–3150 cm^{-1} is assigned to N-H symmetrical stretching of the ethylenediamine (en) ligands, which reflect the valence states of the Pt ions (i.e., electronic state of $[-\text{Pt}(\text{en})_2\text{-I-Pt}(\text{en})_2\text{-I}]_n$) and hydrogen bonding with water of crystallization.¹⁰ X-ray crystal structure of lipid complexed $[\text{Pt}(\text{en})_2\text{Br}_2][\text{Pt}(\text{en})_2]$ reported by Yamashita et al. shows that water of crystallization is hydrogen-bonded with both of the ethylenediamine (en) ligand and lipid sulfonate group.¹¹

The pristine indigo-colored sample shows a $\nu(\text{N-H})$ band at ~ 3090 cm^{-1} , while the $\nu(\text{N-H})$ band of the MeOH-exposed red sample shows splitting into peaks (~ 3070 and ~ 3110 cm^{-1} , peak positions are shown by broken red lines). These observations are consistent with the role of water of crystallization that holds both the regular alignment of close-packed lipid molecules and one-dimensionally densely packed, indigo-colored $[\text{Pt}(\text{en})_2\text{I}_2][\text{Pt}(\text{en})_2]$ complexes by the hydrogen-bond networks. When the lipid complex $[\text{Pt}(\text{en})_2][\text{Pt}(\text{en})_2\text{I}_2](\mathbf{1})_4$ is exposed to MeOH vapor, the water of crystallization present in the lipid complex is kinetically replaced by the excess MeOH vapor, which cannot remain in the lipid complex because, unlike water molecules, they cannot form

bridging hydrogen bonding with ethylenediamine ligands and sulfonate head groups of the lipids. The splitting of the $\nu(\text{N-H})$ band to ~ 3070 and $\sim 3110\text{ cm}^{-1}$ upon contact with MeOH vapor indicates that the densely packed $[\text{Pt}(\text{en})_2][\text{Pt}(\text{en})_2\text{I}_2]$ chain is loosened, and the distance between $\text{Pt}(\text{en})_2$ complexes are elongated to give the charge localized CT state $[-\text{Pt}^{\text{II}}(\text{en})_2-\text{I}-\text{Pt}^{\text{IV}}(\text{en})_2-\text{I}]_n$

This picture is fully consistent with all experimental data, including changes in CT absorption, IR, and Raman spectra shown in Figure 2 and XRD patterns (Fig. 3), and provides the molecular mechanism for the supramolecular vapochromism.

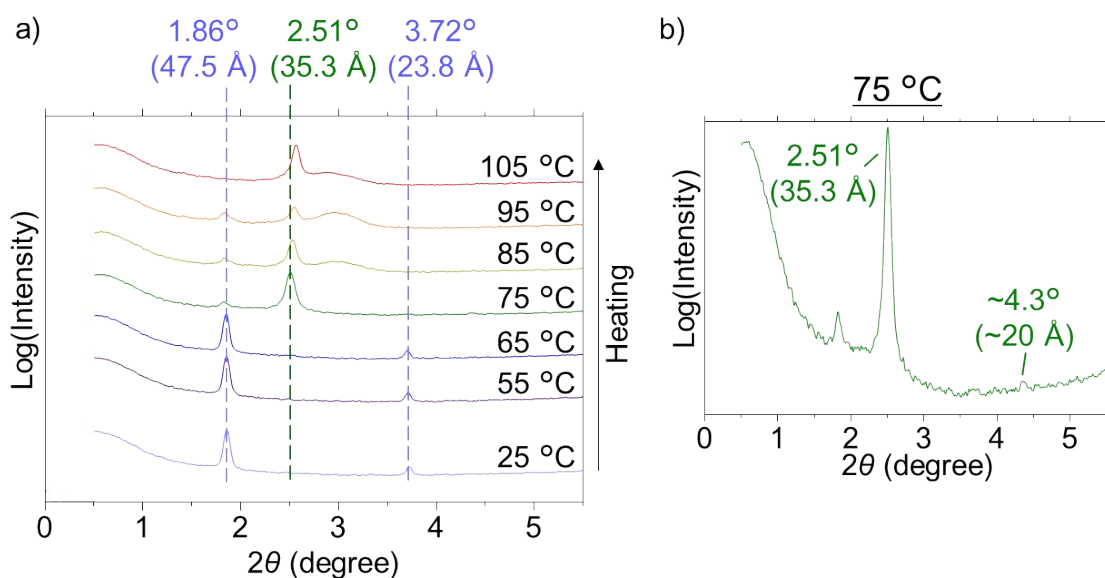


Fig. S11 Variable-temperature SAXS of the complex $[\text{Pt}(\text{en})_2][\text{Pt}(\text{en})_2\text{I}_2](\mathbf{1})_4$ powder (X-ray source: Cu $K\alpha$, transmission geometry), a) diffraction pattern changes upon heating from 25 to 105 °C, b) enlarged view of the diffraction pattern at 75 °C.

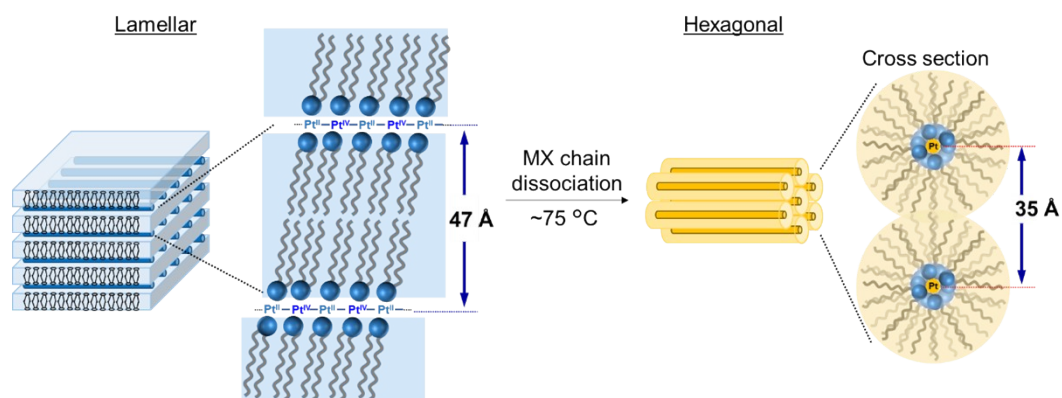


Fig. S12 Schematic illustration of the thermally induced structural changes in lipid-packaged mixed-valence complex $[\text{Pt}(\text{en})_2][\text{Pt}(\text{en})_2\text{I}_2](\mathbf{1})_4$.

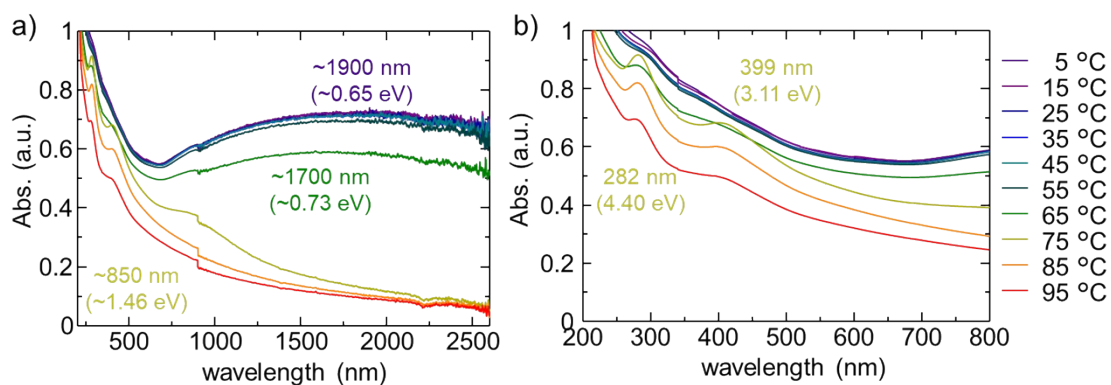


Fig. S13 a) Variable-temperature UV-Vis-NIR spectra of cast film $[\text{Pt}(\text{en})_2][\text{Pt}(\text{en})_2\text{I}_2](\mathbf{1})_4$ and b) its enlarged view in the UV-Vis region. The cast film was prepared at room temperature and then cooled to 5 °C. The absorption spectra were measured during heating from 5 °C to 95 °C.

The thermal desorption of water molecules occurs in concert with changes in the structure of the 1D complex and the orientation of the lipid molecules, as shown by the temperature-dependence of CT spectra and differential scanning calorimetry (DSC). In UV-Vis-NIR spectroscopy, the intensity of broad NIR absorption disappeared in the temperature range of 60-80 °C, which is consistent with the weight loss in TG analysis (Fig. S7a). The heat-induced disappearance of the CT peak is typical of the thermal dissociation of the halogen-bridged 1D structures into the monomer complexes in the film.⁹ This process seems to be promoted by the crystal-to-liquid crystal phase transition of lipid molecules **1**, as indicated by the endothermic peaks observed around 77 °C (Fig. S9a).

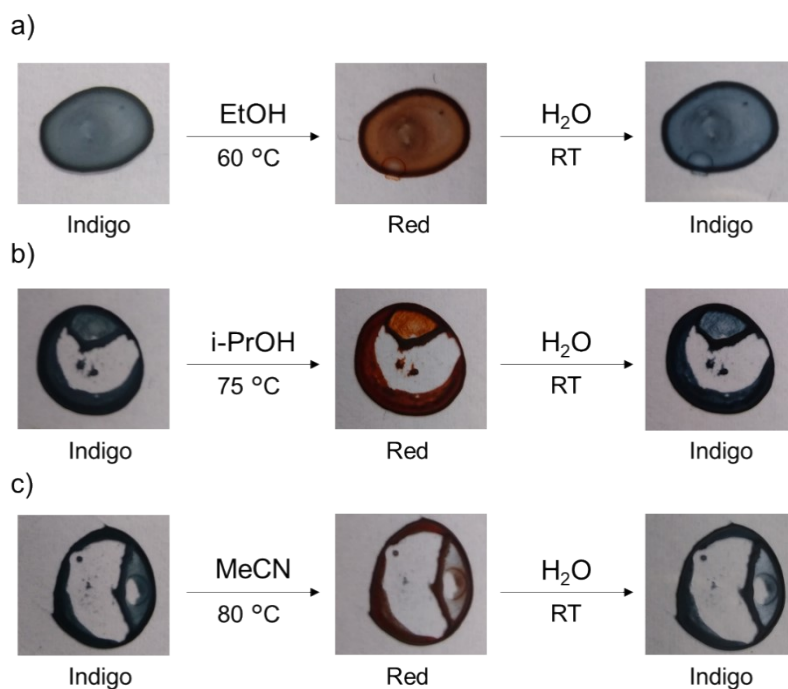


Fig. S14 Reversible color changes of the complex $[\text{Pt}(\text{en})_2][\text{Pt}(\text{en})_2\text{I}_2](\mathbf{1})_4$ induced by polar VOCs and water vapor, a) EtOH, b) i-PrOH, c) MeCN.

[References]

- 1 M. D. Ward and D. A. Buttry, *Science*, **1990**, *249*, 1000–1007.
- 2 C.-S. Lee, Y. Hatanaka and N. Kimizuka, *Int. J. Nanosci.*, **2002**, *01*, 391–395.
- 3 Y. Wada, T. Mitani, M. Yamashita and T. Koda, *J. Phys. Soc. Japan*, **1985**, *54*, 3143–3153.
- 4 N. Kimizuka, *Adv. Mater.*, 2000, **12**, 1461–1463.
- 5 M. Shin, S. Takaishi, S. Kumagai, Y. Ueda, B. K. Breedlove, H. Matsuzaki, H. Okamoto, Y. Wakabayashi and M. Yamashita, *Dalt. Trans.*, **2013**, *42*, 6277–6280.
- 6 B. L. Bracewell, B. L. Scott, M. Berkey and B. I. Swanson, *Synth. Met.*, **1997**, *86*, 2097–2098.
- 7 D. Kawakami, M. Yamashita, S. Matsunaga, S. Takaishi, T. Kajiwara, H. Miyasaka, K. Sugiura, H. Matsuzaki, H. Okamoto, Y. Wakabayashi and H. Sawa, *Angew. Chemie Int. Ed.*, **2006**, *45*, 7214–7217.
- 8 S. Takaishi, M. Takamura, T. Kajiwara, H. Miyasaka, M. Yamashita, M. Iwata, H. Matsuzaki, H. Okamoto, H. Tanaka, S. Kuroda, H. Nishikawa, H. Oshio, K. Kato and M. Takata, *J. Am. Chem. Soc.*, **2008**, *130*, 12080–12084.
- 9 L. Chang-Soo and N. Kimizuka, *Proc. Natl. Acad. Sci.*, **2002**, *99*, 4922–4926.
- 10 H. Okamoto and M. Yamashita, *Bull. Chem. Soc. Jpn.*, **1998**, *71*, 2023–2039.
- 11 S. Kumagai, H. Iguchi, S. Takaishi, B. K. Breedlove, M. Yamashita, H. Matsuzaki, H. Okamoto, K. Kato and M. Takata, *Inorg. Chem.*, **2014**, *53*, 11764–11769.